Conf-9208188--2

UCRL-JC-113768
PREPRINT

RECEIVED
AUG 09 1993
OSTI

Harmonic Generation at High Intensitites

K. J. Schafer, J. L. Krause and K. C. Kulander

This paper was prepared for submittal to the proceedings of the
NATO Advanced Studies Institute
Cargese, Corsica, France
August 17–29, 1992

June 1993

Lawrence Livermore National Laboratory

This is a preprint of a paper intended for publication in a journal or proceedings. Since changes may be made before publication, this preprint is made available with the understanding that it will not be cited or reproduced without the permission of the author.

MASTER

DISTRIBUTION OF THIS DOCUMENT IS UNLIMITED

Disclaimer

This document was prepared as an account of work sponsored by an agency of the United States Government. Neither the United States Government nor the University of California nor any of their employees, makes any warranty, express or implied, or assumes any legal liability or responsibility for the accuracy, completeness, or usefulness of any information, apparatus, product, or process disclosed, or represents that its use would not infringe privately owned rights. Reference herein to any specific commercial products, process, or service by trade name, trademark, manufacturer, or otherwise, does not necessarily constitute or imply its endorsement, recommendation, or favoring by the United States Government or the University of California. The views and opinions of authors expressed herein do not necessarily state or reflect those of the United States Government or the University of California, and shall not be used for advertising or product endorsement purposes.

To appear in: *Laser Interaction with Atoms, Solids and Plasma,*
R. More, Ed., Plenum Press, New York (1993).

HARMONIC GENERATION AT HIGH INTENSITIES

K. J. Schafer, J. L. Krause[a] and K. C. Kulander

Physics Department
Lawrence Livermore National Laboratory
Livermore, CA 94550 USA

Introduction

Atomic electrons subject to intense laser fields can absorb many photons, leading either to multiphoton ionization or the emission of a single, energetic photon which can be a high multiple of the laser frequency. The latter process, high-order harmonic generation, has been observed experimentally using a range of laser wavelengths and intensities over the past several years.[1,2] Harmonic generation spectra have a generic form: a steep decline for the low order harmonics, followed by a plateau extending to high harmonic order, and finally an abrupt cutoff beyond which no harmonics are discernible. During the plateau the harmonic production is a very weak function of the process order. Harmonic generation is a promising source of coherent, tunable radiation in the XUV to soft X-ray range which could have a variety of scientific and possibly technological applications. Its conversion from an interesting multiphoton phenomenon to a useful laboratory radiation source requires a complete understanding of both its microscopic and macroscopic aspects. By "microscopic" we mean the response a single atom to a pulse of intense laser radiation, while "macroscopic" refers to the spatial and temporal characteristics of the emitted radiation as it propagates through the nonlinear medium in which it is produced. In this article we focus on the response of a single atom to an intense, short pulse laser. The macroscopic aspects of harmonic generation are treated in detail elsewhere in this volume.[3]

The most detailed experimental studies of harmonic generation to date used 1μm, 36 psec laser pulses and rare gas atoms at a pressure of ~ 15 torr.[4] The intensity was close to the saturation intensity for the neutral atom, a few times 10^{13} W/cm^2. The maximum harmonic observed ranges from 21st in xenon to the 33rd in argon. (An earlier study by McPherson, *et al.*[5] observed 17th harmonic of a KrF laser (248 nm) in neon at a saturation intensity of ~ 5×10^{15} W/cm^2.) Recently, short-pulse experiments by several groups have observed high-order harmonic generation in the rare gases at intensities well above the saturation intensity for the atom and several of its ionization stages. These experiments have dramatically expanded the range of harmonic generation, converting photons with energies of 1-5 eV to

over 150 eV. L'Huillier and Balcou observed the 125th harmonic of 1064 nm in neon and helium,[6] Macklin, et al. the 111th harmonic of 806 nm in neon,[7] Miyazaki and Sakai the 41st of 616 nm in helium,[8] Crane, *et al.* the 45th harmonic of 527 nm in helium,[9] and Sarukura, et al. have observed the 25th harmonic of 248 nm in neon and helium.[10] Since ionized electrons cannot contribute to harmonic production unless their motion becomes relativistic, these experiments are probing the limits of harmonic generation from neutral atoms. They also raise the question of whether the ions formed during the leading edge of the laser pulse can also contribute to harmonic generation.

In this paper we present some recent results on the response of single atoms at intensities relevant to the short pulse experiments discussed above. The calculations employ time-dependent methods, which we briefly review in the next section. Following that we discuss the behavior of the harmonics as a function of laser intensity. Two features are notable: the slow scaling of the harmonic intensities with laser intensity, and the rapid variation in the phase of the individual harmonics with respect to harmonic order. We then give a simple empirical formula that predicts the extent of the plateau for a given ionization potential, wavelength and intensity. The formula is widely applicable and has recently received experimental confirmation.[6,7] We also discuss a simple classical argument for the size of the cutoff. Following a brief discussion of the connection between harmonic generation and above threshold ionization, we close by commenting on the likelihood that recent experiments have observed harmonic generation from ions.

Numerical Methods

In this section we briefly sketch the numerical methods used to obtain the response of a single atom to an intense laser. Considerably more details can be found in the references.[11,12] Given that the laser field strengths achievable in current short pulse experiments can match or exceed the intra-atomic forces, we need a formalism which can handle these interactions on an equal footing. During the past few years we have developed such an intense field theory. It involves the explicit solution of the time-dependent Schrödinger equation for the atom in the pulsed field. Because the field is extremely strong, it can be represented by a classical oscillating electric field, so that the resulting equation to be solved is given by

$$i\frac{\partial\Psi(r,t)}{\partial t} = \{H_o + f(t)\,z\,E_{\max}\sin(\omega t)\}\Psi(r,t) \tag{1}$$

where H_0 is the atomic Hamiltonian which includes the kinetic energies and the Coulombic interactions. The atom-field interaction term corresponds to a linearly polarized laser field with an slowly varying envelope given by $f(t)$. This is an initial value problem with the field-free ground state of the atom being the solution at $t = 0$.

For one electron atoms or model one-electron potentials we solve Eq. 1 exactly on a numerical grid. For multi-electron atoms this is not possible using present computational capabilities for the optical wavelengths and high intensities of interest here. However, we have demonstrated that a sufficiently accurate solution for the rare gases can be obtained using a single-active-electron (SAE) model.[13] In this approximation simultaneous, multiple excitations of the atomic electrons are neglected. We separately determine the response to the driving field of each valence-shell electron in the potential generated by the nuclear attraction and the remaining electrons, frozen in their initial orbitals. This results in solving an equation similar to Eq. 1 but with an appropriate single-particle effective potential for the orbital of each "active" electron. From the evolution of the time-dependent orbitals we can extract the rates and strengths of the desired electron and photon emission processes.

We determine the value of the time-dependent electronic orbitals on a grid of points defined in either a cylindrical or spherical coordinate system. The linear polarization of the

laser field means the wave function has cylindrical symmetry and therefore only two spatial dimensions are involved. The kinetic energy operations are carried out using finite differences and the time propagation via a Peacemann-Rachford implicit scheme.[12] The development of the SAE model has made possible the study of strongly non-perturbative processes with modest computational effort. Its success demonstrates that the ionization and polarization dynamics of the rare gases become dominated by single excitations in the strong field regime.[14,15]

We follow the evolution of the time-dependent wave function for a pulse, $f(t)$, which rises over five to ten optical cycles then is held constant over many additional cycles. During the constant intensity portion of the pulse, emission rates can be determined. The photon emission strength is given by the square of the Fourier transform of the time-dependent dipole of the total electronic charge distribution:[16]

$$\sigma(\omega) \equiv \omega^3 |d(\omega)|^2 = \omega^3 \left| \frac{1}{T_2 - T_1} \int_{T_1}^{T_2} dt\, e^{i\omega t} \int d^3r\, \Psi^*(\vec{r},t)\, z\, \Psi(\vec{r},t) \right|^2 \tag{2}$$

$$= \omega^{-1} \left| \frac{1}{T_2 - T_1} \int_{T_1}^{T_2} dt\, e^{i\omega t} \int d^3r\, \Psi^*(\vec{r},t)\, \ddot{z}\, \Psi(\vec{r},t) \right|^2 \tag{2'}$$

where z is the coordinate operator along the polarization axis and $\ddot{z} = [H,[H,z]]$ is the acceleration form of the dipole. This latter choice is found to be more tractable because it weights the value of the wave function near the origin which is more likely to be uncontaminated by numerical errors. The use of the acceleration form has allowed us to obtain converged harmonic emission spectra for much higher intensities than would have been possible with Eq. 2. For the hydrogen atom, $\ddot{z}$ is simply $-z/r^3 + f(t)\, E_{max} \sin(wt)$. Because the entire electronic wave function appears in the dipole moment expression we must sum the contributions of the individual active electrons before transforming and squaring, i.e., the separate dipoles add coherently. The interval for the transform is chosen to be well after the turn-on to minimize transient effects. Eq. 2 provides the emission spectrum for a given intensity and wavelength. Because the atoms within the laser focus experience a range of intensities during the pulse, these calculations must be repeated for many intensities. For driving laser pulses shorter than 50 fs the transform in Eq. 2 is taken over the entire pulse because under these circumstances the transient effects are real and can be significant.

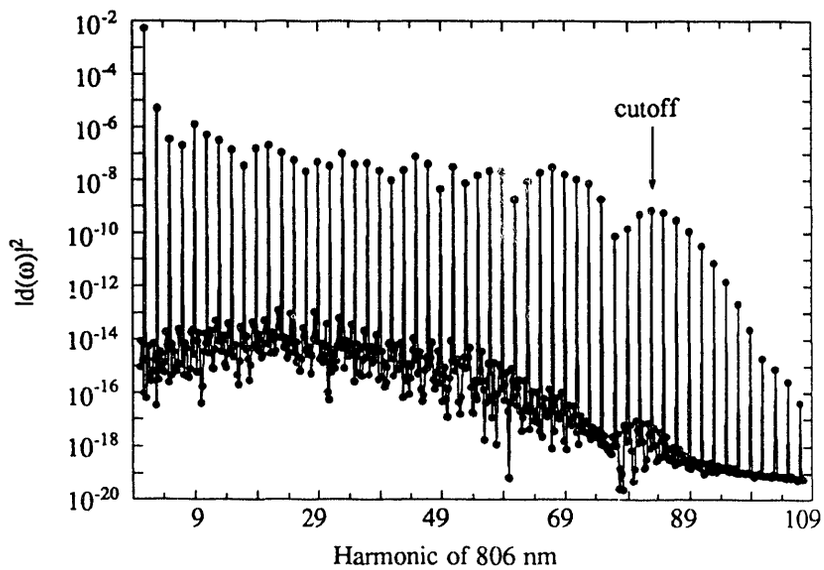

Fig. 1. Single atom spectrum for neon at 806 nm and 6×10^{14} W/cm^2.

Single Atom Results

In this section we examine some of the details of the single atom response to a strong laser field. In Fig. 1 a typical single atom spectrum for neon at an intensity slightly less than saturation for the Stanford experiments[7] is shown. The harmonics appear well above a broad background. The initial decrease, broad plateau, and abrupt cutoff are clearly visible. The cutoff energy is defined as the end of the plateau, i.e. the energy at which the abrupt decline in harmonic intensity begins. It is the scaling with intensity of these features which we concentrate on for the moment.

Fig. 2 shows the intensity dependence for four selected harmonics in hydrogen at 1064 nm. Only the third harmonic behaves perturbatively, scaling as the third power of the intensity. The higher harmonics scale much more slowly than the I^q behavior expected from perturbation theory and show numerous structures. The slow scaling of the harmonics with intensity is responsible for the favorable phase-matching which can be achieved in strong fields, even with tight focusing.[15] The phases of the individual harmonics also show rapid variations with intensity and can vary significantly as a function of harmonic order at a given intensity. This behavior makes it unlikely that several harmonics could be used in concert to form, for example, ultra short pulses.

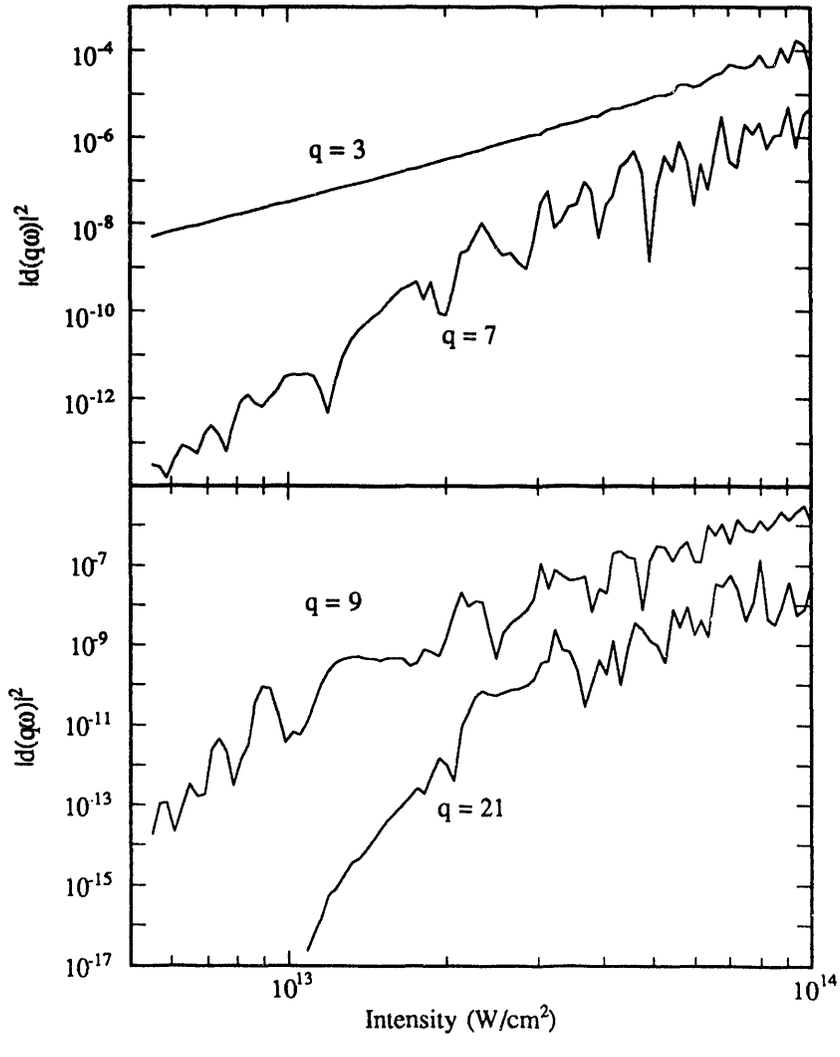

Fig. 2 The intensity dependence of the q=3, 7, 9, and 21 harmonics for hydrogen at 1064 nm.

Figs. 3 (a) and (b) shows single atom spectra for helium at 527 nm and 1053 nm for several intensities between 1-6 x 10^{14} W/cm^2. As the intensity rises, the level of the plateau rises and extends to higher energy. The plateau is somewhat higher for the shorter wavelength, while it extends to higher energy for the longer wavelength. From many such calculations, for a variety of potentials and laser wavelengths, we have found that the cutoff energy obeys the approximate rule:[17]

$$E_c \approx E_o + 3U_p \tag{3}$$

where E_c is the cutoff energy, E_o is the field-free ionization potential of the atom and U_p is the ponderomotive energy for an intensity I, equal to $I/4\omega^2$ in atomic units. The predicted

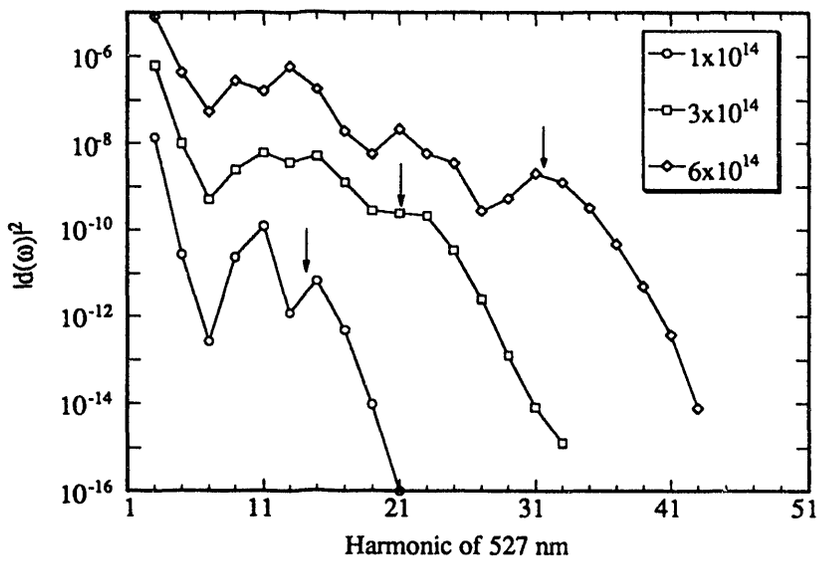

Fig. 3a. Spectrum for helium at 527 nm. Arrows indicate predicted cutoff from Eq. 3.

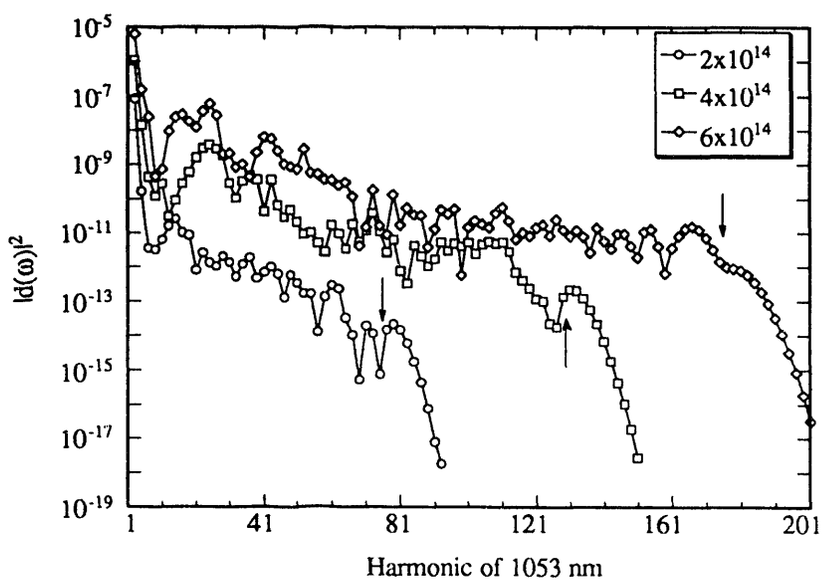

Fig. 3b. Spectrum for helium at 1053 nm. Arrows indicate predicted cutoff from Eq. 3.

cutoff is indicated for each intensity. This cutoff is a simple combination of two energy scales, E_o for the bound state and U_p for free electron motion. We will comment further on the possible origin of the cutoff below. For now, we note the λ^2 dependence of the cutoff would *a priori* tend to favor long wavelength driving lasers for obtaining high energy harmonic photons, however, phase matching considerations may modify this expectation

To illustrate the ubiquitous nature of the cutoff rule, Eq. 3, we examine three potentials that cover a range of conditions. They are: three-dimensional hydrogen, a three dimensional Yukawa-type potential with one bound state, and a one-dimensional "soft Coulomb" potential. The hydrogen potential, $V = -1/r$, has an ionization potential $E_o = 0.5$ au and an infinite number of bound states. The parameters of the Yukawa potential

$$V_{Yukawa} = q' \frac{e^{-\alpha r}}{r} \tag{4}$$

are chosen so that it has the same E_o and only one bound state. It is a short-ranged potential. The one-dimensional "soft-Coulomb" potential, popularized by Eberly and coworkers[18] is given by

$$V(x) = \frac{-1}{\sqrt{\mu + x^2}}. \tag{5}$$

Choosing the parameter μ to be precisely 2 makes the ionization potential equal to that of the hydrogen atom, 0.5 au.[19] This potential is long ranged, supporting an infinite number of bound states in a Rydberg-like series. There is not, however, any correlation between the low-lying excited states of the two Coulombic potentials. Since all three potentials, different as they are, have the same ionization potential, Eq. 3 predicts that for the same wavelength and intensity they will all have the same cutoff. As Fig. 4 shows, this is indeed the case. Furthermore, the difference in the heights of the plateaus is completely accounted for by the difference in the ionization rates of the respective potentials, caused by their very different polarizabilities. This scaling of the height of the plateau with ionization rate is another general feature of single atom harmonic spectra.

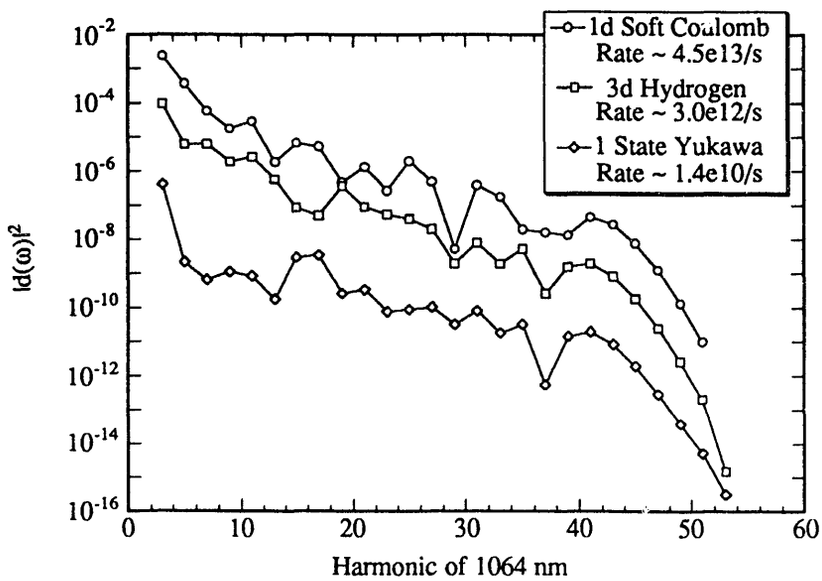

Fig. 4. Single atom spectrum, three different potentials at 1×10^{14} W/cm^2 and 1064nm.

Next we investigate an approximate time-dependent dipole moment which gives some insight into the origin of the high-order harmonics.[20] As noted by Eberly,[21] one can expand the time-dependent dipole in a basis of field-free atomic states, $|n\rangle$:

$$d(t) = \langle \psi(t)|z|\psi(t)\rangle = \sum_{n,m} a_n^*(t) a_m(t) \langle n|z|m\rangle. \tag{6}$$

This expression is still formally exact. If we now assume that the ground state population dominates all of the excited state populations we can approximate $d(t)$ with the single sum

$$d(t) \approx a_o^*(t) \sum_n a_n(t) \langle 0|z|n\rangle + c.c. = \langle \psi(t)|0\rangle\langle 0|z|\psi(t)\rangle + c.c. \tag{7}$$

where $|a_0|^2$ is the field-free ground state population. The physical meaning of this expression is clear: the approximate dipole is the sum of all processes which return the electron to the field-free ground state. When $E_o/\omega >> 1$, the field-free ground state serves as a good approximation to the field-dressed ground state. In Fig. 5 we compare the single atom spectrum computed from the exact and the approximate $d(t)$. The results shown are quite general: we find the spectra agree well for all but the lowest harmonics.[11,20] This demonstrates that the emission of high order harmonics is confined to a small region around the nucleus since the ground state is localized there. This is also the steepest (most anharmonic) part of the potential, resulting in the largest acceleration (cf. Eq. 2').

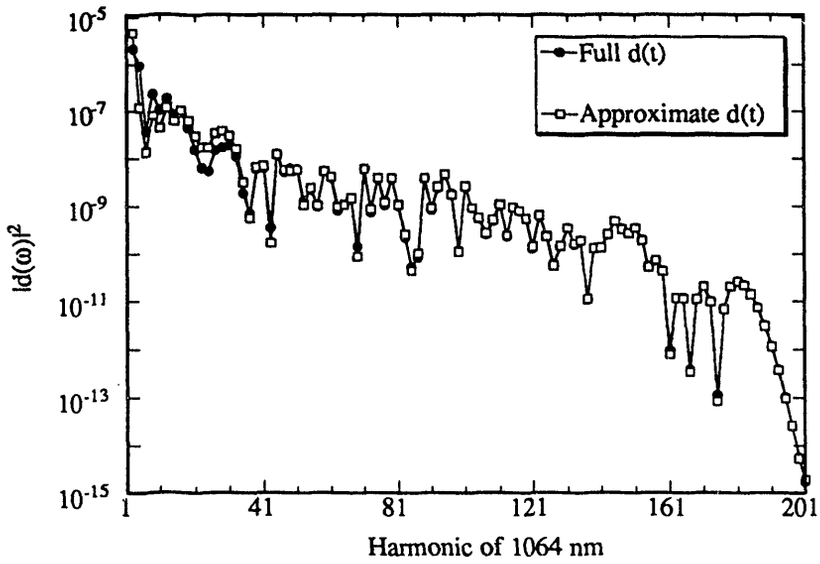

Fig. 5. Single atom spectrum for neon at 6×10^{14} W/cm^2 and 1064 nm using the full and approximate dipole moments.

Simple Classical Model

The realization that high harmonics are emitted as the electron passes the nucleus suggests a natural explanation for the cutoff. If we view the ionization process as liberating some fraction of the electron wave function at each instant of the optical cycle then the atom may be viewed as a "source" of classical electrons that are "born" during the optical cycle. The subsequent motion of the electrons can then be treated classically since they are in the continuum where the density of states is large. The resulting trajectories depend upon the

phase of the electric field at which the electron is assumed to be born, the initial energy (which is probably quite low) and the effect of the atomic potential. The energy of the emitted photons is then obviously limited by the maximum energy that an electron can have at the time it returns to the nucleus. This "two step" model is a simple extension of the classical models proposed for above threshold ionization (ATI) over the past few years.[22-24] These simple models are usually invoked in the tunneling regime, which occurs at high intensities.

To see that this model actually can be predictive, consider electrons that are released at various times during an optical cycle with no initial velocity and ignore the effects of the atomic potential for the moment. The motion of the electron then obeys the one-dimensional equation:

$$x(t) = \alpha_o\left[\sin(\omega t) - \sin(\omega t_o) + \beta - (\omega t - \omega t_o)\cos(\omega t_o)\right] \tag{8}$$

where α_o is the classical electron oscillation amplitude, β is the initial displacement in units of $\alpha_o = E_{max}/\omega^2$ and ωt_o is the initial electric field phase. Fig. 6 is a plot of the energy that the electron has when it returns to the nucleus, in units of U_p, as a function of the initial electric field phase. For this very simplified initial condition the maximum return energy is ~ $3.2U_p$ for an initial phase of 108^0 (the electric field is a maximum for a phase of 90^0). When added to the ionization potential, this predicts the cutoff remarkably well.

It is easy to see several flaws in this simple argument. We have ignored the initial velocity of the electrons. We have also ignored the effect of the potential, which would require that we start the electron with a substantial kinetic energy if it originates at the origin since the potential energy is large and negative there. Most importantly perhaps, the trajectories all originated at the origin which is probably unphysical in the tunneling regime where one would expect the electron to become free at the saddle point of the combined atom + laser potential. This last restriction becomes less important at high intensities since the saddle point occurs quite close to the origin on the scale of α_o. The most that can be said for this "explanation" of the cutoff at this time is that it appears to justify the scale of the observed cutoff and that it is deserving of further study. We are currently investigating the behavior of classical trajectories using more physical initial conditions and taking full account of the atomic potential.[25]

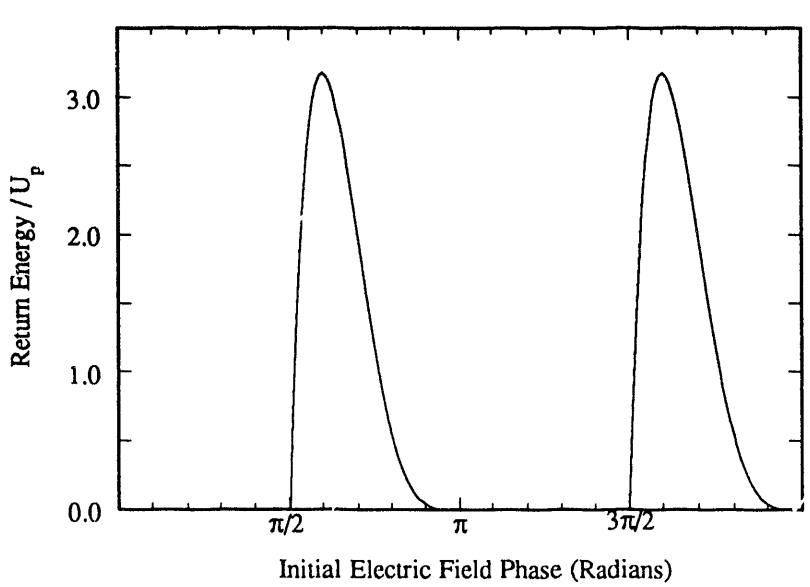

Fig. 6. The energy of a classical electron released at rest from the origin upon its return to the origin as a function of the phase of the electric field at which it was released. A return energy of zero corresponds to a trajectory which never returns.

ATI vs. Harmonics

Several authors have noted the essentially single atom nature of both above threshold ionization and harmonic generation.[20,21] Both originate in the response of a single, strongly driven electron to an oscillating field. It is therefore reasonable to expect that the electron and photon spectra will have similar features. Although this is a fundamental issue in laser-atom interactions, experimental evidence is scarce since electron and photon spectra are usually taken under very different experimental conditions. Due to space charge limitations electron spectra are recorded at very low gas pressures meaning that there is a very limited dynamic range. Harmonic generation spectra are usually recorded at much higher pressure to take advantage of the coherence of the process (i.e., the number of photons scales as the square of the atomic density) and have a much larger dynamic range. Numerical simulations, however allow for the simultaneous calculation of both spectra and hence a direct comparison of the single-atom aspects of ATI and harmonic generation.

Fig. 7 summarizes a series of calculations done for xenon at 1064 nm. The rates are calculated for a specific intensity using a trapezoidal pulse envelope. The harmonic generation spectrum is calculated during the latter portion of the pulse after any transients due to the turn-on have decayed. The ATI rates are given by the probability of finding an electron in a given positive energy state after the laser is off. The most striking result of these single electron calculations is that while the harmonic generation curves show the cutoff we have been discussing, the ATI curves do not. We believe based upon this and similar calculations that the results shown are quite general. The prediction that ATI will smoothly decrease beyond the high harmonic cutoff should become testable in the near future as high repetition rate lasers become available.

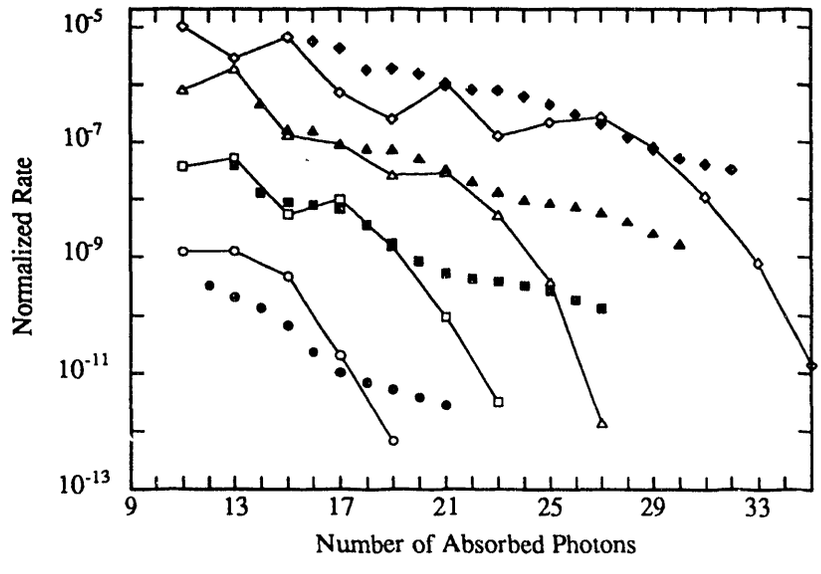

Fig. 7. Single atom harmonic generation (open symbols) and above-threshold ionization (closed symbols) rates for 1064 nm and 1×10^{13} (circles), 2×10^{13} (squares), 3×10^{13} (triangles) and 5×10^{13} (diamonds) W/cm^2.

Harmonic Emission from Ions

In closing we consider the possibility of observing harmonic emission from ions. As peak intensities rise and pulse times become shorter more ions will be exposed to fields strong enough to excite electrons from higher ionization stages. Our calculations to date indicate that most harmonic photons come from neutral atoms.[17] One recent experiment,

however, shows clear evidence for emission from ions. Sarukura *et al.*[10] have reported observation of the 23rd harmonic of 248 nm in He using a 285 fs pulse. We have calculated harmonic spectra for neutral He at this wavelength and find no harmonics beyond the 13th at the saturation intensity, which occurs at about 5×10^{14} W/cm^2. He^+, however, has a saturation intensity of about 4×10^{15} W/cm^2 under these conditions, and is capable of producing the reported harmonics and cutoff. This is illustrated in Fig. 8 where we have scaled the experimental data of Sarukura onto single atom spectra. The cutoffs predicted by Eq. 3 are indicated by arrows as before. This simple exercise neglects phase matching, which is not expected to play a role in determining the cutoff at this wavelength. Similarly, emission from Ne^+ must be invoked to explain the high-order harmonics detected in neon by the same workers. Calculations for helium at 527 nm for 1 psec pulses[17] lead us to believe that single-atom emission from ions can be comparable to that from neutral atoms, although in an experimental laser focus the volume of space occupied by ions may be smaller than that occupied by neutral atoms.

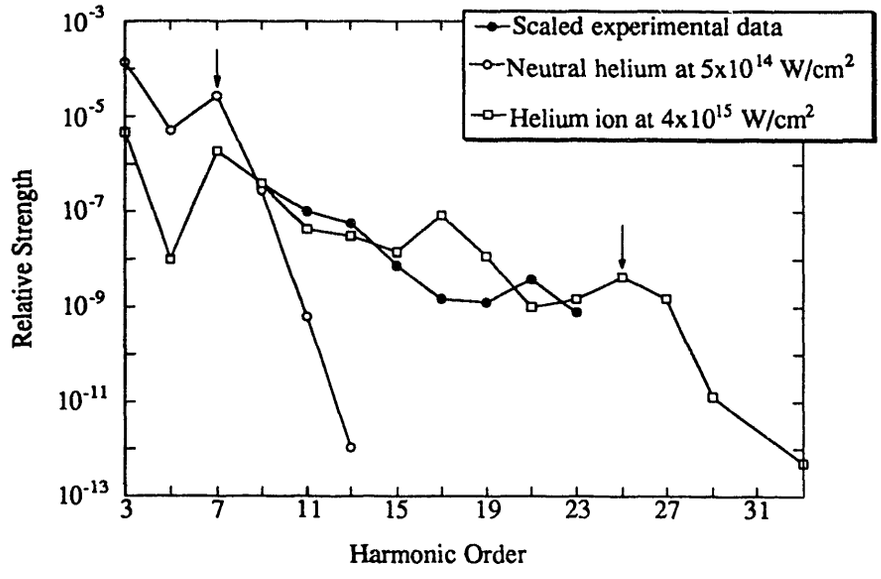

Fig. 8. Single atom spectra for neutral and ionic helium compared to scaled experimental data from Ref. 10. The wavelength is 248 nm.

Acknowledgments

This work has been carried out under the auspices of the U. S. Department of Energy at the Lawrence Livermore National Laboratory under contract number W-7405-ENG-48.

References

(a) Present address: Dept. Of Chemistry, UC San Diego, La Jolla, CA 92093

1. X.F. Li, A. L'Huillier, M. Ferray, L.A. Lompre´ and G. Mainfray, Multiple-harmonic generation in rare gases at ligh laser intensity, *Phys. Rev. A* 39:5751 (1989); Ph. Balcou, C. Cornaggia, A.S.L. Gomes, L.A. Lompre and A. L'Huillier, Optimizing high-order harmonic generation in strong fields, *J. Phys. B* 25:4467 (1992).
2. A. L'Huillier, K.J. Schafer and K.C. Kulander, Theoretical aspects of intense field harmonic generation, *J. Phys. B* 24:3315 (1991).
3. L.A. Lompre´, Harmonic generation in atoms, *in*: "Laser Interaction with Atoms, Solids and Plasma," R. More, ed., Plenum, New York, (1993).

4. A. L'Huillier, Ph. Balcou, S. Candel, K.J. Schafer, and K.C. Kulander, Calculations of high order harmonic generation processes in xenon at 1064 nm, *Phys. Rev. A* 46:2778 (1992).
5. A. McPherson, G. Gibson, H. Jara, U. Johann, T.S. Luk, I. McIntyre, K. Boyer and C.K. Rhodes, Studies of multiphoton vacuum-ultraviolet radiation in rare gases, *J. Opt. Soc. Am. B* 4:595 (1987).
6. A. L'Huillier and Ph. Balcou, High-order harmonic generation in rare gases with a 1 ps 1053-nm laser, *Phys. Rev. Lett.* 70:774 (1993).
7. J.J. Macklin, J.D. Kemetic, and C.L. Gordon, High-order harmonic generation using intense femtosecond pulses, *Phys. Rev. Lett.* 70:766 (1993).
8. K. Miyazaki and H. Sakai, High-order harmonic generation in rare gases with intense subpicosecond dye laser pulses, *J. Phys. B* 25:L83 (1992).
9. J.K. Crane, M.D. Perry, S. Herman and R.W. Falcone, High field harmonic generation in helium, *Optics Letters* 18:1256 (1992).
10. N. Sarukura, K. Hara, T. Adachi, R. Nodormi, M. Watanabe and S. Watanabe, Coherent soft x-ray generation by harmonics of an ultrahigh-power KrF laser, *Phys. Rev. A* 43:1669 (1991).
11. J.L. Krause, K.J. Schafer, and K.C. Kulander, Calculation of photoemission from atoms subject to intense laser fields, *Phys. Rev. A* 45:4998 (1992).
12. K.C. Kulander, K.J. Schafer and J.L. Krause, Time dependent numerical studies of multiphoton processes, *in:* "Atoms in Intense Radiation Fields," M. Gavrila, ed., Advances in Atomic, Molecular and Optical Physics, Supplement 1, Academic Press, New York (1992).
13. K.C. Kulander and T.C. Rescigno, Effective potentials for time-dependent calculations of multiphoton processes in atoms, *Com. Phys. Comm.* 63:523 (1991).
14. K.C. Kulander, Time-dependent Hartree Fock theory of multiphoton ionization: Helium, *Phys. Rev. A* 36:2726 (1987); Time dependent theory of multiphoton ionization of xenon, *Phys. Rev. A* 38:778 (1988).
15. A. L'Huillier, K.J. Schafer, and K.C. Kulander, High order harmonic generation in xenon at 1064 nm: The role of phase matching, *Phys. Rev. Lett.* 66:2200 (1991).
16. K.C. Kulander and B.W. Shore, Calculations of multiple-harmonic conversion of 1064 nm radiation in Xe, *Phys. Rev. Lett.* 62:524 (1989).
17. J.L. Krause, K.J. Schafer, and K.C. Kulander, High-order harmonic generation from atoms and ions in the high intensity regime, *Phys. Rev. Lett.*, 68:3535 (1992).
18. J. Javanainen, J.H. Eberly and Q. Su, Numerical simulations of multiphoton ionization and above-threshold electron spectra, *Phys. Rev. A* 38:3430 (1988).
19. This fact, at first known only via numerical solutions, has been demonstrated analytically. See: W.C. Liu and C.W. Clark, Closed-form solutions of the Schrodinger equation for a model one-dimensional hydrogen atom, *J. Phys. B* 25:L517 (1992).
20. K.J. Schafer, J.L. Krause, and K.C. Kulander, Intense laser-induced nonlinear effects in electron and photon emission from atoms, *Int. J. Nonlinear Optical Physics* 1:245 (1992).
21. J.H. Eberly, Q. Su and J. Javanainen, Nonlinear light scattering accompanying multiphoton ionization, *Phys. Rev. Lett.* 62:881 (1989).
22. H.B. van Linden van den Heuvell and H.G. Muller, Limiting cases of excess-photon ionization, in: "Multiphoton Processes," S.J. Smith and P.L. Knight, eds., Cambridge University Press, Cambridge (1988).
23. T.F. Gallagher, Above-threshold ionization in low-frequency limit, *Phys. Rev. Lett.* 61:2304 (1988).
24. P.B. Corkum, N.H. Burnett and F. Brunel, Above-threshold ionization in the long-wavelength limit, *Phys. Rev. Lett.* 62:1259 (1989).
25. Subsequent study of the classical trajectories has shown that the quasiclassical model does provide a convincing explanation of the harmonic plateau and cutoff. See: K.J. Schafer, K.C. Kulander and J.L. Krause, Classical model for high harmonic cutoff, *Phys. Rev. Lett.* submitted (1993).

END

DATE FILMED

10/12/93